Deconvolving the biogeochemical controls on coral Sr/Ca and Ba/Ca proxies: New perspectives from paired stable Ca, Sr and Ba isotope compositions

Yang Yu[1,2], Ed Hathorne[1], Xuefei Chen[3], Gangjian Wei[3], Florian Böhm[1], Alexander Heuser[1], Anton Eisenhauer[1], Christopher Siebert[1] & Martin Frank[1]

[1] GEOMAR Helmholtz Centre for Ocean Research, Kiel, 24148, Germany
[2] School of Earth and Environmental Sciences, University of St Andrews, St Andrews, KY16 9TS, United Kingdom
[3] State Key Laboratory of Isotope Geochemistry, Guangzhou Institute of Geochemistry, Chinese Academy of Sciences, Guangzhou, 510640, China

Correspondence to: Yang Yu (yy81@st-andrews.ac.uk)

Abstract. This study introduces a novel approach to disentangle the biogeochemical controls on Sr/Ca and Ba/Ca signatures in coral skeletons using paired stable Ca, Sr and Ba isotopes to assess their specific uptake dynamics during coral biomineralization. The observed seasonal variations in stable Ca ($\delta^{44/42}$Ca) and Sr isotopes ($\delta^{88/86}$Sr) underscore the capability of corals to actively mediate the transport of Ca^{2+} and Sr^{2+} ions to the calcifying fluid prior to aragonite precipitation. We suggest that while the individual concentrations of Ca and Sr in the calcifying fluid vary seasonally, the Sr/Ca ratio of the fluid is likely comparable to that of seawater due to similar ion uptake dynamics. In contrast, the observed coral stable Ba isotope compositions ($\delta^{138/134}$Ba) remain essentially constant, suggesting a passive transport mechanism of Ba^{2+} ions, possibly through direct seawater leakage. The contrasting ion transport behaviours of Ba and Ca elucidate the underlying cause of the temperature-dependent variations in coral Ba/Ca records. By evaluating the uptake dynamics of Ca, Sr and Ba via their respective isotope systems, this study provides useful implications for the accurate application of coral Sr/Ca and Ba/Ca as proxies for paleoclimate reconstructions.

1 Introduction

Reef-building corals provide valuable records of past climate conditions, especially in periods and regions where instrumental data are limited (Lea et al., 1989; Beck et al., 1992; Wei et al., 2000; McCulloch et al., 2003). Different coral geochemical proxies have been used to reconstruct ambient seawater properties, such as Sr/Ca for sea surface temperature (SST, Beck et al., 1992), and Ba/Ca for site-specific processes like freshwater input (McCulloch et al., 2003) and upwelling dynamics (Lea et al., 1989). The development of these geochemical proxies typically begins with inorganic precipitation experiments under controlled laboratory settings (e.g., Gaetani and Cohen, 2006; Mavromatis et al., 2018). In such experiments, environmental variables are systematically adjusted to evaluate their individual effects on elemental partitioning between the culturing fluid and aragonite precipitate. In natural environments, however, coral biomineralization fundamentally differs from inorganic

aragonite precipitation due to physiologically mediated ion transport. Unlike inorganic precipitation, coral calcification does not take place directly from seawater but rather from a semi-isolated extracellular calcifying fluid (Cohen and McConnaughey, 2003). While the calcifying fluid originates from the ambient seawater, its chemical compositions is affected by the selective transport of different ions (Gattuso et al., 1999; Cohen and McConnaughey, 2003; Al-Horani et al., 2003; Allemand et al., 2004; Allison et al., 2011; S. Tambutté et al., 2011; Gagnon et al., 2012).

To date, studies on ion transport during coral biomineralization have mainly focused on the uptake of Ca into the calcifying fluid. The delivery of Ca^{2+} ions to the fluid is thought to involve both a passive step through Ca channels and an energy-requiring step via Ca-ATPase pumps (Al-Horani et al., 2003). This two-step mechanism elevates Ca concentrations in the fluid and thus leads to oversaturation with respect to $CaCO_3$ precipitation (Cohen and McConnaughey, 2003; Allemand et al., 2004). Direct microsensor measurements have confirmed that corals can actively raise the concentration of Ca^{2+} ions in the fluid above that in surrounding seawater to facilitate aragonite precipitation (Al-Horani et al., 2003; Sevilgen et al., 2019). This active transport mechanism may also be crucial for the transport of other ions, but the ability to measure and quantify the fluxes of trace elements is limited by the technical challenges of microsensor measurements.

An alternative way to gain insights into the distributions of trace elements is based on the observed skeletal chemistry. However, this method is complicated by the fact that most geochemical proxies rely on elemental ratios that include both trace element and Ca concentrations. For example, the Sr/Ca ratio in coral skeletons exhibits a strong negative correlation with SST and is thus widely used as a paleothermometer (Smith et al., 1979; Beck et al., 1992). Although it is generally accepted that the partitioning of Sr/Ca between aragonite skeleton and calcifying fluid is temperature dependent (Smith et al., 1979; Gaetani and Cohen, 2006), the composition of the fluid may be altered from that of the surrounding seawater by selective ion uptake. In addition, Rayleigh fractionation occurring during aragonite precipitation might further modify the composition of the remaining fluid (e.g., Sinclair and Risk, 2006; DeCarlo et al., 2016). Therefore, the observed skeletal Sr/Ca records may partly reflect variations in the Sr/Ca ratios of the calcifying fluid rather than solely changes in SST. Similarly, coral Ba/Ca ratios have been applied to reconstruct river runoff (McCulloch et al., 2003), dust deposition (Bryan et al., 2019) and oceanic upwelling (Lea et al., 1989), depending on the sources of excess Ba to surface waters. Despite that Ba^{2+} has chemical properties similar to Ca^{2+} given that both are alkaline earth metals, it is not clear if Ba^{2+} follows the same transport pathway as Ca^{2+} ions during coral biomineralization.

To overcome the limitations of using elemental ratios to trace the uptake dynamics of Ca, Sr and Ba, we employ their individual stable isotope systems ($\delta^{44/42}Ca$, $\delta^{88/86}Sr$ and $\delta^{138/134}Ba$) to unravel the biogeochemical controls on their distributions during coral biomineralization. It has been proposed that stable Ca isotope fractionation is physiologically mediated and thus provides valuable insights into Ca uptake dynamics (Inoue et al., 2015; Chen et al., 2016). For example, Böhm et al. (2006) suggested that the active process of transcellular Ca uptake mainly drives the observed temperature-dependent fluctuations in skeletal

$\delta^{44/42}$Ca signatures. Similar to Ca, an incubation study on the scleractinia coral *Acropora verweyi* using the radiotracer ^{85}Sr indicated that the uptake of Sr is also modulated by temperature (Reynaud et al., 2004). In contrast, Ba, a non-biologically essential element, shows little temperature-dependent isotope fractionations across multiple *Porites* colonies (Liu et al., 2019; Hsieh et al., 2022).

Despite the fact that stable Ca, Sr and Ba isotopes are increasingly used as independent proxies for biological and/or environmental parameters, no study has to date integrated these three isotope systems to compare the uptake dynamics of different ions into coral skeletons. Considering their similar chemical properties as alkaline earth elements but different biological functions, the joint examination of their stable isotope compositions and elemental ratios presents a novel approach to evaluate the nature and extent of the biomineralization controls on coral geochemical proxies.

2 Materials and Methods

2.1 Study area and coral sample collection

The South China Sea (SCS) is situated between the Pacific and Indian Oceans, with Xisha Island positioned approximately 600 km southwest of the Pearl River estuary (Fig. 1). This area is dominated by the South Asian monsoon system, with south-westerly winds during summer and north-easterly winds during winter (Wei et al., 2000). These seasonal wind reversals drive corresponding shifts in surface ocean circulation, forming a cyclonic gyre in winter and an anticyclonic gyre in summer (Wong et al., 2007). The observed SST shows an annual average value of 27 °C, ranging from 23 °C in January to 30 °C in June (Tseng et al., 2005).

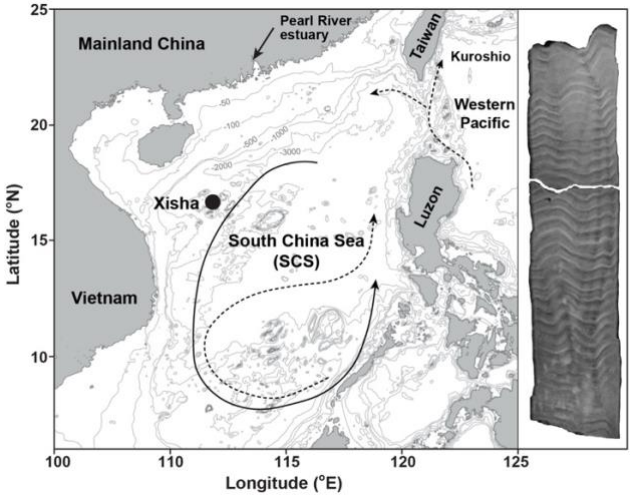

Figure 1: Map of the South China Sea (SCS) illustrates the location of coral sampling site in Xisha (black dot). Ocean circulation patterns reveal a basin-wide cyclonic gyre in winter (solid line) and an anticyclonic gyre in summer (dashed line, Wong et al., 2007). The Kuroshio current and its intrusions into the northern SCS are also indicated with dashed

lines (Wong et al., 2007). In addition, an X-ray image of a sectioned coral core is displayed on the right side of the figure. The map was generated using the Ocean Date View software (Schlitzer, 2009) and modified after Cao et al. (2020).

In 2015, a living *Porites lutea* coral was drilled at Xisha Island (Fig. 1). The coral core was subsequently sectioned into slabs that are perpendicular to its vertical axis of growth. X-ray imaging of the sectioned coral cores reveals distinct high- and low-density bands, corresponding to annual growth increments (Fig. 1). Guided by these annual density bands, sub-samples (~ 0.5 mg) from the upper section of the coral slab were collected along the main growth axis to obtain an approximately monthly resolution. The dissolution of sub-samples was carried out by immersing the powdered carbonate in Milli-Q water and adding drops of 1 M acetic acid stepwise. Brief ultrasonic agitation was used to enhance the dissolution process, allowing for complete dissolution of coral aragonite as gently as possible (Yu et al., 2022).

2.2 Geochemical analysis

The determination of trace element/Ca ratios in the coral samples was conducted at GEOMAR using a standard-sample bracketing method with an Agilent 7500ce ICP-MS. A matrix-matched standard was used to correct for instrumental mass bias and matrix effects as outlined by Yu et al. (2022). The solutions were diluted to a final Ca concentration of 20 ppm. Approximately 0.5 mL solution (~ 10 μg Ca) was consumed for each analysis. Measured intensities were blank corrected and normalised to ^{43}Ca before calculating the element/Ca ratios following the technique of Rosenthal et al. (1999). Coral reference material JCp-1 was analysed as an unknown, yielding mean values of 8.80 ± 0.04 (1SD) mmol/mol for Sr/Ca and 7.28 ± 0.15 (1SD) μmol/mol for Ba/Ca, which are consistent with the values reported by Hathorne et al. (2013).

Coral skeletal carbon isotopes ($\delta^{13}C$) analyses were conducted at GEOMAR using a Finnigan MAT 253 mass spectrometer connected to a Kiel IV Carbonate device system. For carbon isotopic analysis, 200 μg of aragonite samples were reacted with anhydrous 105% H_3PO_4 under vacuum at 70 °C to release CO_2. Carbon isotopic compositions are reported in δ notation as per mil (‰) deviation from the Vienna Pee Dee Belemnite (VPDB) standard. Calibration to the VPDB scale was achieved using the National Bureau of Standards (NBS) 19 and an in-house standard (Std Bremen). The analytical precision for $\delta^{13}C$ measurements was better than 0.10‰ (2SD, N = 34).

Stable Ca isotope analyses were performed at GEOMAR using a Thermo Fisher Neptune Plus MC-ICP-MS, following the protocols outlined by Eisenhauer et al. (2019). An aliquot of the dissolved sample containing approximately 50 μg of Ca was used for chemical purification. Instrumental mass fractionation was corrected using a standard-sample bracketing method with an in-house Ca standard solution. Stable Ca isotope compositions are reported in per mil (‰) relative to the NIST SRM 915a Ca standard as $\delta^{44/42}Ca$ (‰) = $(^{44/42}Ca_{sample}/^{44/42}Ca_{NIST\ SRM\ 915a} - 1) \times 1000$. Repeated analyses of NIST SRM 1486 (–0.50 ± 0.04‰, 2SD), NIST SRM 915b (0.34 ± 0.04‰, 2SD) and IAPSO seawater standard (0.93 ± 0.02‰, 2SD) showed good

agreement with published values (Hippler et al., 2003; Heuser and Eisenhauer, 2008; Tacail et al., 2014; Heuser et al., 2016). The long-term reproducibility (2SD) for all analysed reference materials was better than 0.04‰.

Stable Sr isotope measurements were performed on a Finnigan Triton TIMS at GEOMAR, following the methods described by Krabbenhöft et al. (2009). The ^{87}Sr-^{84}Sr double spike was added to one aliquot containing ~250 ng Sr before chemical separation while the other remained un-spiked. Sr was purified from the matrix elements using Eichrom Sr-spec resin, achieving a recovery rate of over 90%. Stable Sr isotope compositions are reported relative to the NIST SRM 987 Sr standard as $\delta^{88/86}Sr$ (‰) = $(^{88/86}Sr_{sample}/^{88/86}Sr_{NIST\ SRM\ 987} - 1) \times 1000$. The coral JCp-1 standard was analysed repeatedly, yielding an average $\delta^{88/86}Sr$ value of 0.20 ± 0.02‰ (2SD, N = 10), consistent with published value of 0.197 ± 0.008‰ (2SE, Krabbenhöft et al., 2009). The long-term analytical error on JCp-1 and IAPSO seawater standards is 0.02‰ (2SD).

Stable Ba isotope analyses of coral samples were conducted at GEOMAR using a Neptune Plus MC-ICP-MS, following the methods detailed by Yu et al. (2020). A sample volume corresponding to approximately 50 ng of Ba was mixed with the ^{130}Ba-^{135}Ba double spike to correct for instrumental mass fractionation. Ba was purified twice from the matrix elements using 1.4 mL of Bio-Rad AG 50W-X8 resin. Stable Ba isotope measurements were conducted at a matrix tolerance state defined by a high Normalized Ar Index value (NAI, which is an index of plasma temperature, Fietzke and Frische, 2016; Yu et al., 2024, 2020). Stable Ba isotope compositions are reported relative to the NIST SRM 3014a Ba standard as $\delta^{138/134}Ba$ (‰) = $(^{138/134}Ba_{sample}/^{138/134}Ba_{NIST\ SRM\ 3104a} - 1) \times 1000$. Repeated analyses of coral reference material JCp-1 yielded a $\delta^{138/134}Ba$ value of 0.29 ± 0.04‰ (2SD, N = 12), which agrees well with reported values (Horner et al., 2015; Pretet et al., 2015; Hemsing et al., 2018; Zeng et al., 2019; Geyman et al., 2019; Cao et al., 2020, 2021; Yu et al., 2022). The long-term reproducibility (2SD) is 0.03‰ for JCp-1 coral standard and 0.04‰ for seawater reference materials.

2.3 Coral age model

The distinct annual cycles in the observed skeletal Sr/Ca data were used to establish the chronology of the Xisha coral core. The seasonal maxima and minima of coral Sr/Ca data were correlated with the corresponding seasonal extreme values in the monthly HadISST records (Hadley Centre Global Sea Ice and Sea Surface Temperatures, Rayner et al., 2003). This approach allows for the construction of an age model for the coral core that extends from the year of collection (2015) back to 2004. Note that time series data for the uppermost section of the coral head (2014 - 2015) were excluded from this study, considering the anomalously low Sr/Ca ratios associated with less clearly defined annual density bands as shown in Fig. 1.

3 Results

The skeletal Sr/Ca and Ba/Ca records are shown in Fig. 2 and detailed in Table S1. In addition, two-year records (2007 - 2009) of skeletal Ba isotopes ($\delta^{138/134}Ba$), Ca isotopes ($\delta^{44/42}Ca$) and Sr isotopes ($\delta^{88/86}Sr$) are plotted alongside the corresponding

SST and coral $\delta^{13}C$ data in Fig. 3 and also presented in Table S1. To quantitatively assess the correlations between environmental factors and coral geochemical proxies, we employed the York regression method (York et al., 2004) to account for analytical uncertainties in both variables.

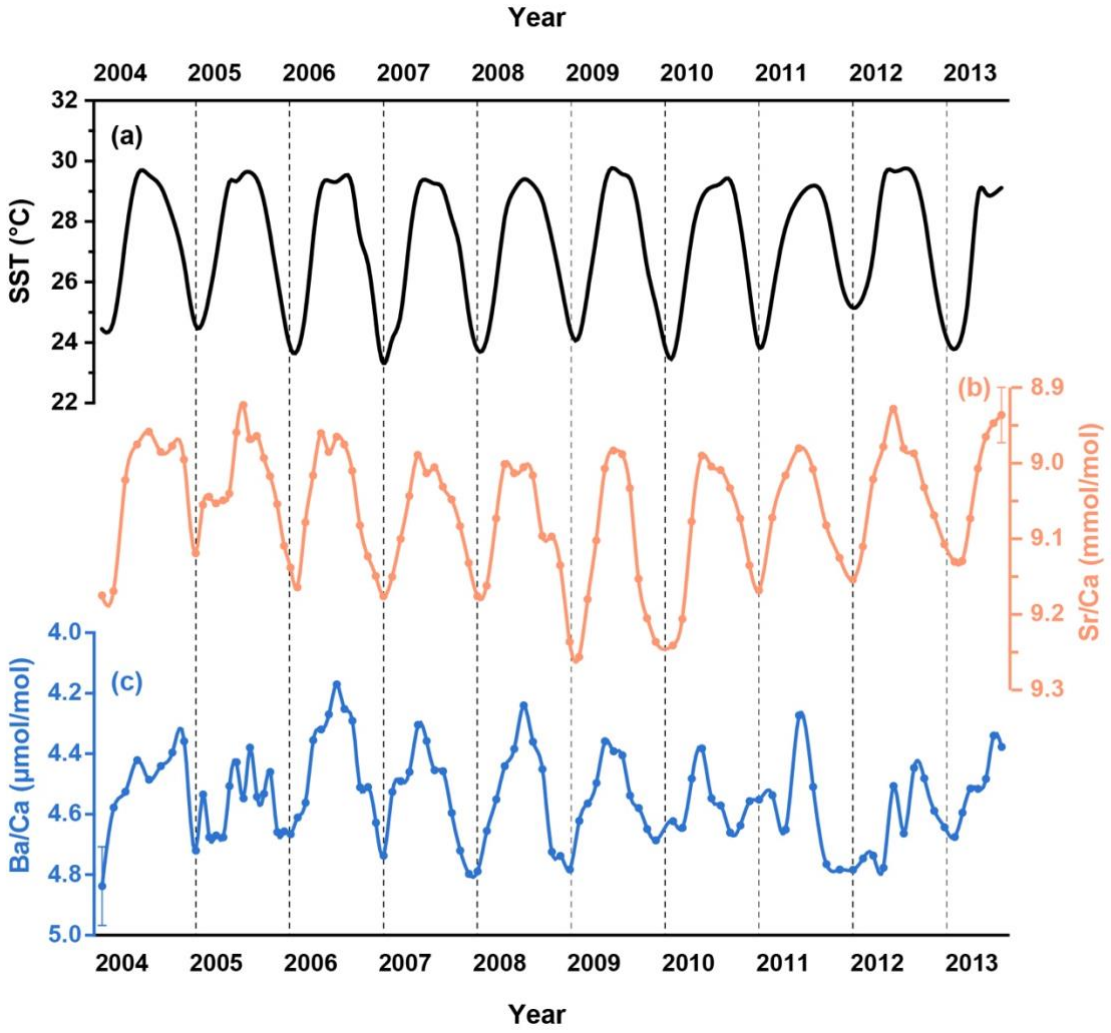

Figure 2: (a) The U.K. Meteorological Office Hadley Centre Global Sea Ice and Sea Surface Temperature (HadISST, Rayner et al., 2013). Monthly resolved coral geochemical data for (b) Sr/Ca and (c) Ba/Ca from the coral samples in the South China Sea.

Coral Sr/Ca ratios exhibit well-defined cyclic fluctuations on a seasonal timescale and show strong agreement with the HadISST dataset ($R^2 = 0.70$, $p < 0.05$) for the period between 2004 and 2013 (Fig. 2b). Coral Ba/Ca data display similar seasonal variations (Fig. 2c) that show a statistically significant correlation with the HadISST dataset ($R^2 = 0.36$, $p < 0.05$). The skeletal $\delta^{13}C$ variability generally tracks the seasonal cycles displayed by SST, with higher $\delta^{13}C$ values accompanying

elevated SST (Fig. 3c). The time series data for coral $\delta^{138/134}$Ba (Fig. 3e) show negligible variations over the two-year period of coral growth and do not exhibit any correlation with SST ($R^2 = 0.03$, $p > 0.05$). In contrast, the time series data for coral skeletal $\delta^{44/42}$Ca (Fig. 3f) exhibit small but well-resolved seasonal fluctuations that align well with changes in SST (Fig. 4a, $R^2 = 0.26$, $p < 0.05$). Similar to Ca isotopes, coral skeletal $\delta^{88/86}$Sr (Fig. 3g) displays clear seasonal variations that show a statistically significant correlation with SST (Fig. 4b, $R^2 = 0.30$, $p < 0.05$), with consistently lower $\delta^{88/86}$Sr values during summer months and higher $\delta^{88/86}$Sr values during winter months. This includes a notable decline in $\delta^{88/86}$Sr during the summer of 2008, coinciding with elevated SST and increased δ^{13}C values.

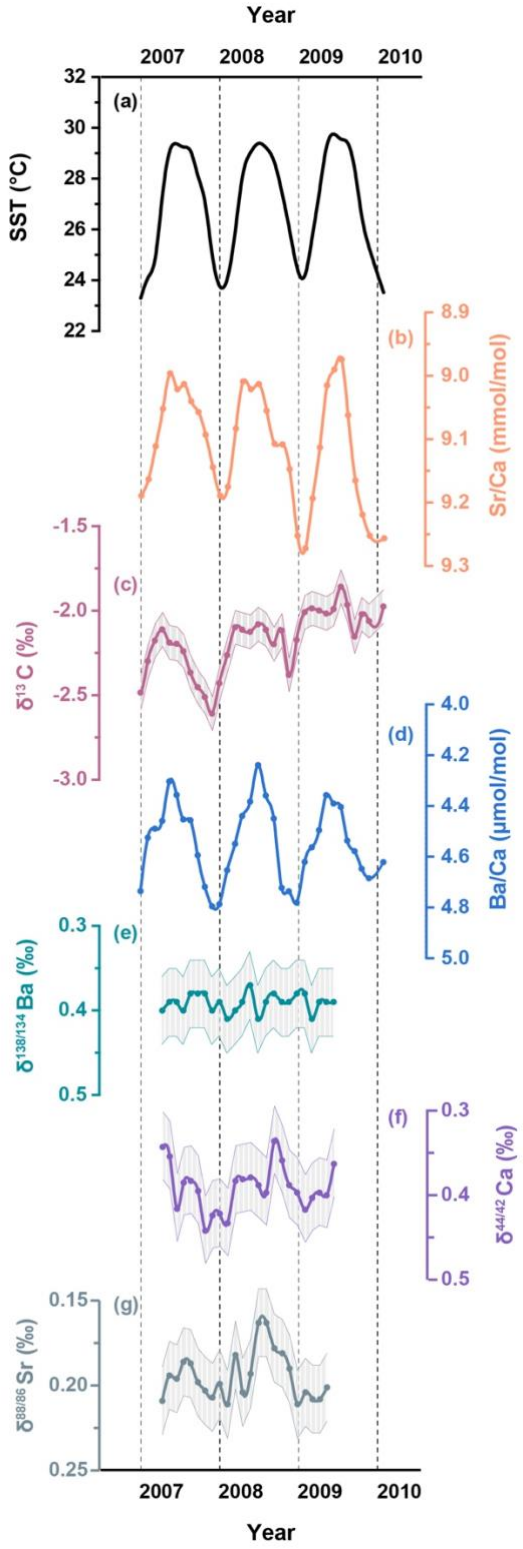
Year
2007
2008
2009
2010
(a)
SST (°C)
32
30
28
26
24
22
(b)
Sr/Ca (mmol/mol)
8.9
9.0
9.1
9.2
9.3
(c)
δ13C (‰)
-1.5
-2.0
-2.5
-3.0
(d)
Ba/Ca (μmol/mol)
4.0
4.2
4.4
4.6
4.8
5.0
(e)
δ138/134Ba (‰)
0.3
0.4
0.5
(f)
δ44/42Ca (‰)
0.3
0.4
0.5
(g)
δ88/86Sr (‰)
0.15
0.20
0.25
2007
2008
2009
2010
Year

Figure 3: A two-year record (2007-2009) of (a) the U.K. Meteorological Office Hadley Centre Global Sea Ice and Sea Surface Temperature (HadISST, Rayner et al., 2013), and skeletal geochemical data for (b) Sr/Ca; (c) $\delta^{13}C$; (d) Ba/Ca; (e) $\delta^{138/134}Ba$; (f) $\delta^{44/42}Ca$; (g) $\delta^{88/86}Sr$ from the coral samples in the South China Sea. Shaded bands represent analytical uncertainties (2SD) for each dataset.

4 Discussion

4.1 Surface seawater chemistry

The SCS is a semi-enclosed marginal sea situated between the Asian continent and the western Pacific Ocean, strongly affected by the seasonal Asian monsoon circulation (Fig. 1). Given that the relatively long residence time of Ca (~ 1 Ma) and Sr (~ 4 Ma) in seawater (Drever, 1988), dissolved Ca and Sr concentrations in surface seawater are expected to be constant on seasonal timescales. In contrast, terrestrial input from river runoff, such as the Pearl River, serves as a major source of excess Ba to the nearshore SCS (Cao et al., 2021). However, our coral sampling site is geographically remote (~ 600 km, Fig. 1) from the Pearl River discharge plume and thus is unlikely to be influenced by terrestrial Ba contributions. In addition, the observed coral Ba/Ca ratios are consistently high during the dry winter monsoon periods (Fig. 2c), indicating that neither precipitation nor runoff can account for the regular Ba/Ca peaks in dry seasons.

Apart from riverine inputs, the observed Ba/Ca peaks are potentially related to the advection of the Kuroshio Branch Water from the North Pacific during the winter monsoon (Fig. 1). However, no evidence of such contributions can be found in the surface Ba concentrations ([Ba]) in the SCS, which has surface [Ba] values similar to those observed in the western North Pacific (Bacon and Edmond, 1972; Monnin et al., 1999). Furthermore, dissolved stable Ba isotope compositions in the surface seawater of the SCS sampled in January are characterised by a value of 0.63 ± 0.04‰ (Cao et al., 2020), which is comparable to those observed in the open Pacific sampled in September (0.64 ± 0.03‰, Hsieh and Henderson, 2017). Therefore, we suggest that water mass advection has a negligible effect on the distinct seasonal patterns observed in coral Ba/Ca.

It has been shown that increased wind speeds during the northeast monsoon enhance vertical mixing (Tseng et al., 2005). Although Xisha is located outside the main upwelling areas, the influence of wind-driven vertical mixing is reflected in seasonal fluctuations of the mixed layer depth (MLD). Within the coral sampling area, the MLD is relatively shallow (20 - 40 m) during the summer monsoon and markedly deeper (~ 90 m) during the winter monsoon (Tseng et al., 2005). Consequently, the entrainment of deeper waters with higher [Ba] would be expected in winter as a result of the nutrient-like depth profile of dissolved [Ba] in water column (Monnin et al., 1999b). However, the vertical distributions of dissolved [Ba] are essentially constant within the upper 150 m in the SCS (Cao et al., 2020), suggesting that the intensified wind-induced mixing and the consequent MLD deepening are unlikely to explain the observed seasonal variations in coral Ba/Ca. Therefore, we propose that the seasonal fluctuations in coral skeletal Ba/Ca and Sr/Ca ratios are not driven by changes in surface seawater compositions.

4.2 Uptake dynamics of ions

4.2.1 Ca^{2+} ion transport

During the processes of Ca transport in corals, there are likely two stages of Ca transport where its stable isotopes ($\delta^{44/42}Ca$) could potentially undergo fractionation (Böhm et al., 2006). In the first stage, Ca channels permit passive diffusion of seawater Ca^{2+} ion into cells (Allemand et al., 2011). Considering coral channels have relatively narrow pores, the large, hydrated seawater Ca^{2+} ions must be dehydrated at the channel entrance before being transported into the cell interior (S. Tambutté et al., 2011). In the second stage, the cell exports the Ca^{2+} ions into the extracellular calcifying fluid via the active Ca-ATPase pumps (Allemand et al., 2011). This step requires energy to move Ca^{2+} ions against their concentration gradient, leading to high Ca^{2+} concentration in the fluid to form $CaCO_3$ (S. Tambutté et al., 2011).

The observed monthly resolved coral $\delta^{44/42}Ca$ values are typically lower during summer months associated with elevated SST, resulting in a statistically significant ($p < 0.05$) negative correlation between $\delta^{44/42}Ca$ and SST (Fig. 4a, solid circles). This negative correlation between temperature and coral Ca isotope fractionation differs from results of previous studies. For example, Böhm et al. (2006) identified a significant ($p < 0.05$) but positive correlation between $\delta^{44/42}Ca$ and temperature in both cultured *Acropora* and open ocean *Porites* and *Pavona* corals (Fig. 4a, empty circles). Similarly, coral culturing experiments also found a positive correlation between the mean skeletal $\delta^{44/42}Ca$ of *Porites* colonies and temperature (Fig. 4a, empty squares, Inoue et al., 2015).

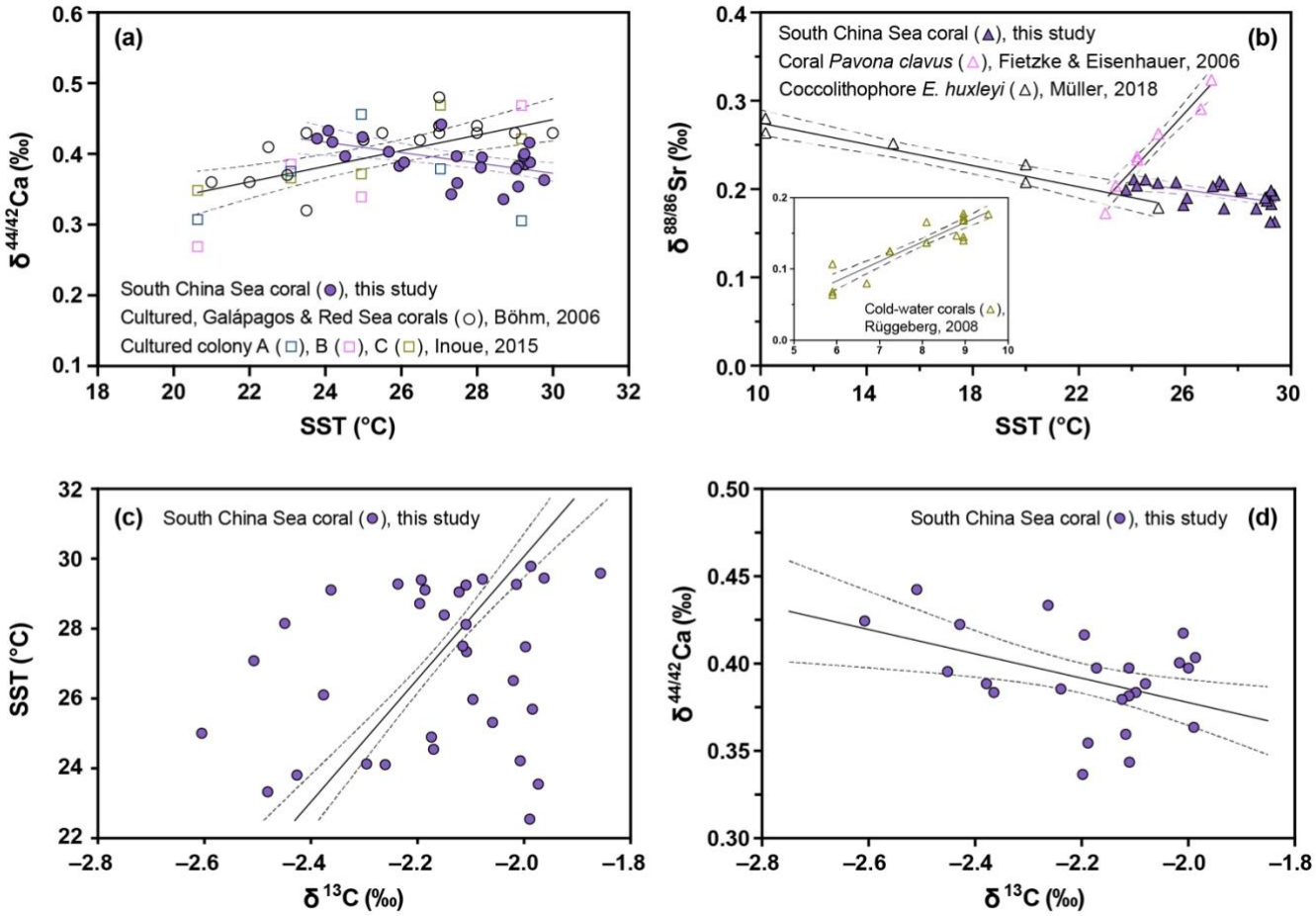

Figure 4: (a) Correlations between $\delta^{44/42}$Ca and SST for the South China Sea coral (solid circles), the cultured, Galápagos and Red Sea corals (empty circles, Böhm et al., 2006), and three different cultured coral colonies (empty squares, Inoue et al., 2015); (b) Correlations between $\delta^{88/86}$Sr and SST for the South China Sea coral (solid triangles in purple), coral *Pavona clavus* (empty triangles in pink, Fietzke & Eisenhauer, 2006), coccolithophore *E. huxleyi* (empty triangles in black, Müller et al., 2018), and cold-water corals *L. pertusa* (empty triangles in olive drab, Rüggeberg et al., 2008); (c) Correlation between SST and δ^{13}C for the South China Sea coral; (d) Correlation between $\delta^{44/42}$Ca and δ^{13}C for the South China Sea coral.

According to inorganic precipitation models (e.g., Gussone et al., 2003), an increase in temperature drives the fractionation factor between the calcifying fluid and the aragonite skeleton toward unity. This thermodynamic effect should diminish the isotopic selection between ^{42}Ca and ^{44}Ca, resulting in less pronounced Ca isotope fractionation (i.e. higher skeletal $\delta^{44/42}$Ca values) as temperature increases. Additionally, ion dehydration models by Mejía et al. (2018) and Hofmann et al. (2012) suggest that higher temperatures weaken the hydration shell around Ca ions, lowering the energy barrier for dehydration. This thermodynamic effect also reduces isotope fractionation and leads to a positive correlation between $\delta^{44/42}$Ca and temperature.

However, our results show a contrasting negative correlation between $\delta^{44/42}Ca$ and temperature (Fig. 4a). We propose that as temperature rises, corals likely accelerate its metabolic flux of ions to sustain enhanced calcification. To maintain these rapid transport rates, Ca-ATPase pumps and channels likely amplify their preference for lighter Ca isotopes that require less energy to dehydrate. Consequently, this metabolically driven kinetic fractionation progressively dominates over the thermodynamic response, resulting in the observed negative correlation between skeletal $\delta^{44/42}Ca$ and SST.

In line with our suggestion, we observe an increase in skeletal $\delta^{13}C$ in the summer months, resulting in a significant ($p < 0.05$) positive correlation between $\delta^{13}C$ and SST (Fig. 4c). The preferential utilization of the light carbon isotope (^{12}C) by zooxanthellae during photosynthesis results in an increased concentration of $^{13}CO_2$ in the pool of inorganic carbon accessible for coral calcification. The formation of coral skeleton during periods of intense photosynthetic activity is thus associated with higher skeletal $\delta^{13}C$ values (McConnaughey et al., 1997; Felis et al., 1998). The negative correlation between skeletal $\delta^{13}C$ and $\delta^{44/42}Ca$ ($p < 0.05$, Fig. 4d) indicates that the increased rate of active ion transport and enhanced Ca isotope fractionation is fuelled by the energy supplied by photosynthesis of zooxanthellae.

While previous studies have reported positive correlations between SST and $\delta^{44/42}Ca$ (Böhm et al., 2006; Inoue et al., 2015), the contrasting negative pattern observed here highlights the significant role of coral physiology on Ca transport. Because different coral species and even individual colonies can exhibit distinct metabolic responses to environmental factors, the temperature dependence of Ca isotope fractionation may vary depending on specific environmental conditions and physiological states. Considering that our study focuses on a single *Porites* colony within a relatively warm environment, we hypothesise that elevated SST largely stimulates metabolic activity and induces a highly efficient, rate-driven Ca isotope fractionation. This interpretation is consistent with the specific findings of Inoue et al. (2015) for "Colony A", which showed a breakdown of the positive trend and a shift towards lighter $\delta^{44/42}Ca$ values at temperatures above 24 °C. Similarly, the positive correlation reported by Böhm et al. 2006 appears to be less defined at the higher end of their temperature range.

4.2.2 Sr^{2+} ion transport

Similar to Ca, the time series data for coral skeletal $\delta^{88/86}Sr$ (Fig. 3g) display clear seasonal changes over a continuous two-year period, with consistently lower $\delta^{88/86}Sr$ values in summer months and higher $\delta^{88/86}Sr$ values in winter months. As the magnitude of Sr isotope fractionation increases (i.e. lower $\delta^{88/86}Sr$ values) with rising SST, the negative $\delta^{88/86}Sr$-temperature relationship observed in this study differs from previous studies (Fig. 4b). For example, both Fietzke and Eisenhauer (2006) and Rüggeberg et al. (2008) reported a positive relationship between $\delta^{88/86}Sr$ and temperature in inorganic aragonite, shallow- and cold-water corals (Fig. 4b). However, subsequent studies found either very muted variability in in coral $\delta^{88/86}Sr$ or no clear positive temperature dependence (Raddatz et al., 2013; Fruchter et al., 2016).

Considering the similar chemical properties and ionic radius of Sr^{2+} and Ca^{2+} (Shannon, 1976), both ions are likely transported and fractionated via a similar biologically-mediated pathway. An incubation study using the radiotracer ^{85}Sr indicated that the uptake of Sr is a function of temperature and follows the same pattern as Ca uptake (Reynaud et al., 2004). The significant ($p < 0.05$) negative correlation observed in the $\delta^{88/86}$Sr-SST plot (Fig. 4b) suggests that the variations in $\delta^{88/86}$Sr are likely regulated by the temperature-dependent uptake of Sr^{2+} ions. A similar significant negative correlation of $\delta^{88/86}$Sr and temperature has been reported in culturing experiments on coccolithophores, where a larger fractionation in $\delta^{88/86}$Sr was observed at elevated temperature (Fig. 4b, Müller et al., 2018). This negative relationship between coccolithophore $\delta^{88/86}$Sr and temperature (Fig. 4b) is consistent with previous results obtained for three different coccolithophore species (Stevenson et al., 2014).

Unlike corals, coccolithophores as unicellular organisms with intra-cellular calcification, exclusively use trans-membrane transport, whereas corals may use a combination of transcellular and paracellular transport mechanisms (Hohn and Merico, 2015). Despite that the relative contribution of the paracellular transport to coral Sr uptake is largely unknown, the similarity of Sr isotope fractionation patterns between the strictly transcellular coccolithophores and our coral record indicates that Sr is transported primarily via active transcellular pathways in corals. As elevated SST accelerates the metabolic flux required to sustain rapid calcification, transport enzymes likely favour lighter Sr isotopes due to their more rapid dehydration kinetics and lower activation energy for desolvation. The coherent negative temperature dependence of both Sr and Ca isotope fractionation in our coral record indicates a shared, metabolically-dominated active transport mechanism.

4.2.3 Ba^{2+} ion transport

Compared to Sr^{2+} (1.31 Å), the Ba^{2+} ion is characterised by a significantly larger ionic radius (1.47 Å) than that of Ca^{2+} ion (1.18 Å), with a difference of approximately 25% (Shannon, 1976). This substantial difference in ion radius may prevent Ba from using the same transcellular pathway as Ca (Gaetani and Cohen, 2006). In addition, Ba is a non-essential element for biological processes and can be toxic to organisms at elevated concentrations (Kravchenko et al., 2014), indicating that Ba is less likely to be regulated and transported by the active transcellular pathway. More importantly, the essentially invariant fractionation behaviours of stable Ba isotopes implies that the incorporation of Ba^{2+} ions differ from that of Ca^{2+} ion (Fig. 3e).

The results of our study indicate that stable Ba isotope fractionation between coral skeletons and seawater (0.63 ± 0.04‰, Cao et al., 2020) is constant at a calculated value of –0.24 ± 0.05‰. This fractionation factor is generally comparable with the reported factor of –0.30‰ in the SCS (Liu et al., 2019), and an average value of –0.28 ± 0.06‰ from multiple *Porites* colonies located near Singapore (Hsieh et al., 2022). Like Ca and Sr, the stable Ba isotope fractionation can be attributed to the weaker ion-water bond of lighter isotopes (e.g., ^{134}Ba) compared to heavier isotopes (e.g., ^{138}Ba) during the processes of ion

dehydration. The observed constant coral $\delta^{138/134}$Ba signatures indicate that Ba uptake and associated isotope fractionation are likely controlled by a mechanism that is largely independent of changes in environmental factors.

Experiments using membrane impermeant fluorescent dye-tracer, such as calcein, have indicated the existence of a paracellular pathway by which seawater may bypasses the cytoplasm, and directly enter the calcifying fluid (Allemand et al., 2011; E. Tambutté et al., 2011; Gagnon et al., 2012). This paracellular route facilitates diffusive or advective exchange of ions between the calcifying fluid and the surrounding seawater. A recent culturing experiment on the incorporation of anions into coral skeletons provides additional support for direct transport of seawater to the fluid (Ram and Erez, 2023). Therefore, we suggest that this paracellular pathway and Ba dehydration likely dominate the Ba transport and its isotope fractionation during coral biomineralization, respectively.

Considering that the ionic radius of Ca^{2+} is smaller than that of Ba^{2+}, it is possible that seawater Ca^{2+} ions may also enter the coral calcifying fluid directly via the paracellular pathway. However, the paracellular pathway relies on the Ca concentration gradient between seawater and the fluid, but currently available data suggest higher Ca concentrations in the fluid compared to seawater (Al-Horani et al., 2003; Sevilgen et al., 2019). In addition, the paracellular pathway allows for passive diffusion or advection, which does not require any energy cost. In contrast, the transcellular transport requires ATP to actively move ions against their concentration gradients into the fluid (S. Tambutté et al., 2011). We assume that during periods of elevated SST, the Ca channels and Ca-ATPase pumps become more active in supplying Ca^{2+} ions via the transcellular pathway. In contrast, the transport of non-essential Ba^{2+} ions is primarily governed by the passive paracellular transport that is less sensitive to SST changes. As a result, the uptake of Ca increases more at higher SST, while Ba uptake remains more stable and does not respond much to temperature changes. Therefore, the seasonal variations in the observed Ba/Ca ratios of the coral skeleton are likely driven by changes in the flux of Ca^{2+} ions rather than that of Ba^{2+} ions. The contrasting ion transport behaviours between Ba and Ca elucidates the mechanism underlying seasonal variations in coral Ba/Ca and $\delta^{44/42}$Ca, while also accounting for the invariable coral $\delta^{138/134}$Ba records.

4.3 Implications for coral geochemical proxies.

Although the empirical correlation between coral Sr/Ca ratios and SST has been widely used for the establishment of high-resolution SST records (Smith et al., 1979; Beck et al., 1992), a major uncertainty arises from the potential for corals to actively modulate the incorporation of trace elements into the calcifying fluid prior to aragonite precipitation. The seasonal fluctuations observed in coral skeleton $\delta^{44/42}$Ca and $\delta^{88/86}$Sr indicate that Ca and Sr concentrations in the fluid could vary over seasonal timescales, likely driven by changes in environmental factors like SST and related coral physiological processes. However, if Sr flux changes linearly with Ca flux as SST varies, then their elemental ratio (i.e. Sr/Ca) in the calcifying fluid remains relatively constant despite absolute changes in concentrations of both ions. Therefore, the temporal fluctuations in the uptake

rates of Sr and Ca ions are unlikely to explain the observed monthly changes in skeletal Sr/Ca ratios. Instead, the temperature-sensitive partitioning of Sr and Ca into coral aragonite is likely the primary driver of seasonal variations in skeletal Sr/Ca records. This result supports the wealth of empirical results demonstrating coral Sr/Ca ratios provide a reliable proxy for reconstructing past SST.

On the other hand, the limited Ba isotope fractionation suggests that the concentration of Ba in the fluid is nearly constant and does not respond strongly to SST changes. The elevated Ca concentrations in the fluid, driven by enhanced transport of Ca^{2+} ions, likely account for the seasonal variations in skeletal Ba/Ca records observed. Culturing experiments have shown that coral Ba/Ca ratios vary in response to temperature and light conditions, even when seawater Ba concentrations are kept constant (Yamazaki et al., 2021; Sakata et al., 2024). These observations demonstrate that elevated temperature or light intensity, both of which can enhance coral metabolic activity, likely drive the changes in skeletal Ba/Ca ratios through their influence on Ca transport dynamics. Therefore, this metabolic component of coral Ba/Ca needs to be removed to improve the reliability of coral Ba/Ca for tracing past ocean chemistry. In comparison, coral stable Ba isotopes are largely independent from such biological effects, thereby supporting the use of coral $\delta^{138/134}$Ba as a more robust proxy to reconstruct seawater Ba isotope compositions and related geochemical cycling over time.

5 Conclusions

Coral biomineralization consists of two individual steps: Modifications of the extracellular calcifying fluid and subsequent aragonite precipitation. Our monthly resolved coral geochemical records from the South China Sea indicate that the first step of transporting Ca^{2+} and Sr^{2+} ions from seawater to the fluid is tightly regulated by physiological processes and thus exhibits a distinct temperature dependence. This is supported by the corresponding stable Ca and Sr isotope fractionations, showing consistently decreasing $\delta^{44/42}$Ca and $\delta^{88/86}$Sr values with elevated temperatures. Although the respective concentrations of Sr and Ca in the fluid likely fluctuate seasonally, the elemental ratio of Sr/Ca remains constant in the fluid, thus supporting the use of coral Sr/Ca as a proxy for sea surface temperature reconstructions. In contrast, the transport of Ba^{2+} ions likely occurs through a passive mechanism such as seawater leakage, which is independent of environmental factors as evidenced by the invariable coral $\delta^{138/134}$Ba records. Therefore, the different incorporation behaviours of Ba and Ca ions likely drive the observed seasonal variations in coral Ba/Ca records. Overall, our study highlights the complex interplay between biological processes and environmental factors during coral biomineralization, emphasising the importance of understanding the uptake dynamics of different ions for accurate paleoclimate reconstructions.

Data availability

All data are provided in the Supplement.

Author contributions

YY and EH conceived and designed the study; YY and AH performed the analyses; YY carried out the investigation and visualization; YY wrote the manuscript draft; YY, EH, XC, GW, FB, AH, AE, CS, and MF reviewed and edited the manuscript; MF supervised and administered the project; MF acquired funding; XC and GW provided resources.

Competing interests

The authors declare that they have no conflict of interest.

Acknowledgements

Great thanks to Sieglinde Kolbrink and Ana Kolevica for all their support in the laboratory.

Financial support:

The Deutsche Forschungsgemeinschaft (DFG, German Research Foundation) – Project number 468592241 (M.F.) – SPP 2299/Project number 441832482 is acknowledged for financial support of Y. Y. during this study.

References

Al-Horani F. A., Al-Moghrabi S. M. and de Beer D. (2003) The mechanism of calcification and its relation to photosynthesis and respiration in the scleractinian coral Galaxea fascicularis. *Marine Biology* **142**, 419–426.

Allemand D., Ferrier-Pagès C., Furla P., Houlbrèque F., Puverel S., Reynaud S., Tambutté É., Tambutté S. and Zoccola D. (2004) Biomineralisation in reef-building corals: from molecular mechanisms to environmental control. *Comptes Rendus Palevol* **3**, 453–467.

Allemand D., Tambutté É., Zoccola D. and Tambutté S. (2011) Coral Calcification, Cells to Reefs. In *Coral Reefs: An Ecosystem in Transition* (eds. Z. Dubinsky and N. Stambler). Springer Netherlands, Dordrecht. pp. 119–150.

Allison N., Cohen I., Finch A. A. and Erez J. (2011) Controls on Sr/Ca and Mg/Ca in scleractinian corals: The effects of Ca-ATPase and transcellular Ca channels on skeletal chemistry. *Geochimica et Cosmochimica Acta* **75**, 6350–6360.

Bacon M. P. and Edmond J. M. (1972) Barium at Geosecs III in the southwest Pacific. *Earth and Planetary Science Letters* **16**, 66–74.

Beck J. W., Edwards R. L., Ito E., Taylor F. W., Recy J., Rougerie F., Joannot P. and Henin C. (1992) Sea-surface temperature from coral skeletal strontium/calcium ratios. *Science, New Series* **257**, 644–647.

Böhm F., Gussone N., Eisenhauer A., Dullo W.-C., Reynaud S. and Paytan A. (2006) Calcium isotope fractionation in modern scleractinian corals. *Geochimica et Cosmochimica Acta* **70**, 4452–4462.

Bryan S. P., Hughen K. A., Karnauskas K. B. and Farrar J. T. (2019) Two Hundred Fifty Years of Reconstructed South Asian Summer Monsoon Intensity and Decadal-Scale Variability. *Geophys. Res. Lett.* **46**, 3927–3935.

Cao Z., Li Y., Rao X., Yu Y., Hathorne E. C., Siebert C., Dai M. and Frank M. (2020) Constraining barium isotope fractionation in the upper water column of the South China Sea. *Geochimica et Cosmochimica Acta* **288**, 120–137.

Cao Z., Rao X., Yu Y., Siebert C., Hathorne E. C., Liu B., Wang G., Lian E., Wang Z., Zhang R., Gao L., Wei G., Yang S., Dai M. and Frank M. (2021) Stable Barium Isotope Dynamics During Estuarine Mixing. *Geophys Res Lett* **48**.

Chen X., Deng W., Zhu H., Zhang Z., Wei G. and McCulloch M. T. (2016) Assessment of coral δ44/40Ca as a paleoclimate proxy in the Great Barrier Reef of Australia. *Chemical Geology* **435**, 71–78.

Cohen A. L. and McConnaughey T. A. (2003) Geochemical Perspectives on Coral Mineralization. *Reviews in Mineralogy and Geochemistry* **54**, 151–187.

DeCarlo T. M., Gaetani G. A., Cohen A. L., Foster G. L., Alpert A. E. and Stewart J. A. (2016) Coral Sr-U thermometry. *Paleoceanography* **31**, 626–638.

Drever J. I. (1988) *The geochemistry of natural waters*., Prentice hall Englewood Cliffs.

Eisenhauer A., Müller M., Heuser A., Kolevica A., Glüer C.-C., Both M., Laue C., Hehn U. v., Kloth S., Shroff R. and Schrezenmeir J. (2019) Calcium isotope ratios in blood and urine: A new biomarker for the diagnosis of osteoporosis. *Bone Reports* **10**, 100200.

Felis T., Pätzold J., Loya Y. and Wefer G. (1998) Vertical water mass mixing and plankton blooms recorded in skeletal stable carbon isotopes of a Red Sea coral. *Journal of Geophysical Research: Oceans* **103**, 30731–30739.

Fietzke J. and Eisenhauer A. (2006) Determination of temperature-dependent stable strontium isotope (88Sr/86Sr) fractionation via bracketing standard MC-ICP-MS. *Geochemistry, Geophysics, Geosystems* **7**.

Fietzke J. and Frische M. (2016) Experimental evaluation of elemental behavior during LA-ICP-MS: influences of plasma conditions and limits of plasma robustness. *J. Anal. At. Spectrom.* **31**, 234–244.

Fruchter N., Eisenhauer A., Dietzel M., Fietzke J., Böhm F., Montagna P., Stein M., Lazar B., Rodolfo-Metalpa R. and Erez J. (2016) 88Sr/86Sr fractionation in inorganic aragonite and in corals. *Geochimica et Cosmochimica Acta* **178**, 268–280.

Gaetani G. A. and Cohen A. L. (2006) Element partitioning during precipitation of aragonite from seawater: A framework for understanding paleoproxies. *Geochimica et Cosmochimica Acta* **70**, 4617–4634.

Gagnon A. C., Adkins J. F. and Erez J. (2012) Seawater transport during coral biomineralization. *Earth and Planetary Science Letters* **329–330**, 150–161.

Gattuso J.-P., Allemand D. and Frankignoulle M. (1999) Photosynthesis and Calcification at Cellular, Organismal and Community Levels in Coral Reefs: A Review on Interactions and Control by Carbonate Chemistry1. *American Zoologist* **39**, 160–183.

Geyman B. M., Ptacek J. L., LaVigne M. and Horner T. J. (2019) Barium in deep-sea bamboo corals: Phase associations, barium stable isotopes, & prospects for paleoceanography. *Earth and Planetary Science Letters* **525**, 115751.

Gussone N., Eisenhauer A., Heuser A., Dietzel M., Bock B., Böhm F., Spero H. J., Lea D. W., Bijma J. and Nägler T. F. (2003) Model for kinetic effects on calcium isotope fractionation (δ44Ca) in inorganic aragonite and cultured planktonic foraminifera. *Geochimica et Cosmochimica Acta* **67**, 1375–1382.

Hathorne E. C., Gagnon A., Felis T., Adkins J., Asami R., Boer W., Caillon N., Case D., Cobb K. M., Douville E., deMenocal P., Eisenhauer A., Garbe-Schönberg D., Geibert W., Goldstein S., Hughen K., Inoue M., Kawahata H., Kölling M., Cornec F. L., Linsley B. K., McGregor H. V., Montagna P., Nurhati I. S., Quinn T. M., Raddatz J., Rebaubier H., Robinson L., Sadekov A., Sherrell R., Sinclair D., Tudhope A. W., Wei G., Wong H., Wu H. C. and You C.-F. (2013) Interlaboratory study for coral Sr/Ca and other element/Ca ratio measurements. *Geochem. Geophys. Geosyst.* **14**, 3730–3750.

Hemsing F., Hsieh Y.-T., Bridgestock L., Spooner P. T., Robinson L. F., Frank N. and Henderson G. M. (2018) Barium isotopes in cold-water corals. *Earth and Planetary Science Letters* **491**, 183–192.

Heuser A. and Eisenhauer A. (2008) The Calcium Isotope Composition (δ44/40Ca) of NIST SRM 915b and NIST SRM 1486. *Geostandards and Geoanalytical Research* **32**, 311–315.

Heuser A., Schmitt A.-D., Gussone N. and Wombacher F. (2016) Analytical Methods. In *Calcium Stable Isotope Geochemistry* Advances in Isotope Geochemistry. Springer Berlin Heidelberg, Berlin, Heidelberg. pp. 23–73.

Hippler D., Schmitt A.-D., Gussone N., Heuser A., Stille P., Eisenhauer A. and Nägler T. F. (2003) Calcium Isotopic Composition of Various Reference Materials and Seawater. *Geostandards and Geoanalytical Research* **27**, 13–19.

Hofmann A. E., Bourg I. C. and DePaolo D. J. (2012) Ion desolvation as a mechanism for kinetic isotope fractionation in aqueous systems. *Proc. Natl. Acad. Sci. U.S.A.* **109**, 18689–18694.

Hohn S. and Merico A. (2015) Quantifying the relative importance of transcellular and paracellular ion transports to coral polyp calcification. *Frontiers in Earth Science* **2**.

Horner T. J., Kinsley C. W. and Nielsen S. G. (2015) Barium-isotopic fractionation in seawater mediated by barite cycling and oceanic circulation. *Earth and Planetary Science Letters* **430**, 511–522.

Hsieh Y.-T. and Henderson G. M. (2017) Barium stable isotopes in the global ocean: Tracer of Ba inputs and utilization. *Earth and Planetary Science Letters* **473**, 269–278.

Hsieh Y.-T., Paver R., Tanzil J. T. I., Bridgestock L., Lee J. N. and Henderson G. M. (2022) Multi-colony calibration of barium isotopes between shallow-water coral skeletons and in-situ seawater: Implications for paleo proxies. *Earth and Planetary Science Letters* **580**, 117369.

Inoue M., Gussone N., Koga Y., Iwase A., Suzuki A., Sakai K. and Kawahata H. (2015) Controlling factors of Ca isotope fractionation in scleractinian corals evaluated by temperature, pH and light controlled culture experiments. *Geochimica et Cosmochimica Acta* **167**, 80–92.

Krabbenhöft A., Fietzke J., Eisenhauer A., Liebetrau V., Böhm F. and Vollstaedt H. (2009) Determination of radiogenic and stable strontium isotope ratios (87 Sr/ 86 Sr; δ 88/ 86 Sr) by thermal ionization mass spectrometry applying an 87 Sr/ 84 Sr double spike. *Journal of Analytical Atomic Spectrometry* **24**, 1267–1271.

Kravchenko J., Darrah T. H., Miller R. K., Lyerly H. K. and Vengosh A. (2014) A review of the health impacts of barium from natural and anthropogenic exposure. *Environ Geochem Health* **36**, 797–814.

Lea D. W., Shen G. T. and Boyle E. A. (1989) Coralline barium records temporal variability in equatorial Pacific upwelling. *Nature* **340**, 373–376.

Liu Y., Li X., Zeng Z., Yu H.-M., Huang F., Felis T. and Shen C.-C. (2019) Annually-resolved coral skeletal δ138/134Ba records: A new proxy for oceanic Ba cycling. *Geochimica et Cosmochimica Acta* **247**, 27–39.

Mavromatis V., Goetschl K. E., Grengg C., Konrad F., Purgstaller B. and Dietzel M. (2018) Barium partitioning in calcite and aragonite as a function of growth rate. *Geochimica et Cosmochimica Acta* **237**, 65–78.

McConnaughey T. A., Burdett J., Whelan J. F. and Paull C. K. (1997) Carbon isotopes in biological carbonates: Respiration and photosynthesis. *Geochimica et Cosmochimica Acta* **61**, 611–622.

McCulloch M., Fallon S., Wyndham T., Hendy E., Lough J. and Barnes D. (2003) Coral record of increased sediment flux to the inner Great Barrier Reef since European settlement. *Nature* **421**, 727–730.

Mejía L. M., Paytan A., Eisenhauer A., Böhm F., Kolevica A., Bolton C., Méndez-Vicente A., Abrevaya L., Isensee K. and Stoll H. (2018) Controls over δ44/40Ca and Sr/Ca variations in coccoliths: New perspectives from laboratory cultures and cellular models. *Earth and Planetary Science Letters* **481**, 48–60.

Monnin C., Jeandel C., Cattaldo T. and Dehairs F. (1999a) The marine barite saturation state of the world's oceans. *Marine Chemistry* **65**, 253–261.

Monnin C., Jeandel C., Cattaldo T. and Dehairs F. (1999b) The marine barite saturation state of the world's oceans. *Marine Chemistry* **65**, 253–261.

Müller M. N., Krabbenhöft A., Vollstaedt H., Brandini F. P. and Eisenhauer A. (2018) Stable isotope fractionation of strontium in coccolithophore calcite: Influence of temperature and carbonate chemistry. *Geobiology* **16**, 297–306.

Pretet C., Zuilen K., Nägler T. F., Reynaud S., Böttcher M. E. and Samankassou E. (2015) Constraints on barium isotope fractionation during aragonite precipitation by corals. *Depositional Rec* **1**, 118–129.

Raddatz J., Liebetrau V., Rüggeberg A., Hathorne E., Krabbenhöft A., Eisenhauer A., Böhm F., Vollstaedt H., Fietzke J., López Correa M., Freiwald A. and Dullo W.-Chr. (2013) Stable Sr-isotope, Sr/Ca, Mg/Ca, Li/Ca and Mg/Li ratios in the scleractinian cold-water coral Lophelia pertusa. *Chemical Geology* **352**, 143–152.

Ram S. and Erez J. (2023) Anion elements incorporation into corals skeletons: Experimental approach for biomineralization and paleo-proxies. *Proceedings of the National Academy of Sciences* **120**, e2306627120.

Rayner N. A., Parker D. E., Horton E. B., Folland C. K., Alexander L. V., Rowell D. P., Kent E. C. and Kaplan A. (2003) Global analyses of sea surface temperature, sea ice, and night marine air temperature since the late nineteenth century. *Journal of Geophysical Research: Atmospheres* **108**.

Reynaud S., Ferrier-Pagès C., Boisson F., Allemand D. and Fairbanks R. (2004) Effect of light and temperature on calcification and strontium uptake in the scleractinian coral Acropora verweyi. *Mar. Ecol. Prog. Ser.* **279**, 105–112.

Rosenthal Y., Field M. P. and Sherrell R. M. (1999) Precise Determination of Element/Calcium Ratios in Calcareous Samples Using Sector Field Inductively Coupled Plasma Mass Spectrometry. *Anal. Chem.* **71**, 3248–3253.

Rüggeberg A., Fietzke J., Liebetrau V., Eisenhauer A., Dullo W.-C. and Freiwald A. (2008) Stable strontium isotopes (*δ*88/86Sr) in cold-water corals — A new proxy for reconstruction of intermediate ocean water temperatures. *Earth and Planetary Science Letters* **269**, 570–575.

Sakata S., Inoue M., Tanaka Y., Nakamura T., Sakai K., Ikehara M. and Suzuki A. (2024) Assessment of chemical compositions in coral skeletons (Acropora digitifera and Porites australiensis) as temperature proxies. *Front. Mar. Sci.* **11**.

Sevilgen D. S., Venn A. A., Hu M. Y., Tambutté E., De Beer D., Planas-Bielsa V. and Tambutté S. (2019) Full in vivo characterization of carbonate chemistry at the site of calcification in corals. *Sci. Adv.* **5**, eaau7447.

Shannon R. D. (1976) Revised effective ionic radii and systematic studies of interatomic distances in halides and chalcogenides. *Acta Cryst A* **32**, 751–767.

Sinclair D. J. and Risk M. J. (2006) A numerical model of trace-element coprecipitation in a physicochemical calcification system: Application to coral biomineralization and trace-element 'vital effects.' *Geochimica et Cosmochimica Acta* **70**, 3855–3868.

Smith S. V., Buddemeier R. W., Redalje R. C. and Houck J. E. (1979) Strontium-calcium thermometry in coral skeletons. *Science, New Series* **204**, 404–407.

Stevenson E. I., Hermoso M., Rickaby R. E. M., Tyler J. J., Minoletti F., Parkinson I. J., Mokadem F. and Burton K. W. (2014) Controls on stable strontium isotope fractionation in coccolithophores with implications for the marine Sr cycle. *Geochimica et Cosmochimica Acta* **128**, 225–235.

Tacail T., Albalat E., Télouk P. and Balter V. (2014) A simplified protocol for measurement of Ca isotopes in biological samples. *Journal of Analytical Atomic Spectrometry* **29**, 529–535.

Tambutté E., Tambutté S., Segonds N., Zoccola D., Venn A., Erez J. and Allemand D. (2011) Calcein labelling and electrophysiology: insights on coral tissue permeability and calcification. *Proceedings of the Royal Society B: Biological Sciences* **279**, 19–27.

Tambutté S., Holcomb M., Ferrier-Pagès C., Reynaud S., Tambutté É., Zoccola D. and Allemand D. (2011) Coral biomineralization: From the gene to the environment. *Journal of Experimental Marine Biology and Ecology* **408**, 58–78.

Tseng C.-M., Wong G. T. F., Lin I.-I., Wu C.-R. and Liu K.-K. (2005) A unique seasonal pattern in phytoplankton biomass in low-latitude waters in the South China Sea. *Geophysical Research Letters* **32**.

Wei G., Sun M., Li X. and Nie B. (2000) Mg/Ca, Sr/Ca and U/Ca ratios of a porites coral from Sanya Bay, Hainan Island, South China Sea and their relationships to sea surface temperature. *Palaeogeography, Palaeoclimatology, Palaeoecology* **162**, 59–74.

Wong G. T. F., Ku T.-L., Mulholland M., Tseng C.-M. and Wang D.-P. (2007) The SouthEast Asian Time-series Study (SEATS) and the biogeochemistry of the South China Sea—An overview. *Deep Sea Research Part II: Topical Studies in Oceanography* **54**, 1434–1447.

Yamazaki A., Yano M., Harii S. and Watanabe T. (2021) Effects of light on the Ba/Ca ratios in coral skeletons. *Chemical Geology* **559**, 119911.

York D., Evensen N. M., Martínez M. L. and De Basabe Delgado J. (2004) Unified equations for the slope, intercept, and standard errors of the best straight line. *Am. J. Phys.* **72**, 367–375.

Yu Y., Hathorne E., Siebert C., Felis T., Rajendran C. P. and Frank M. (2022) Monthly resolved coral barium isotopes record increased riverine inputs during the South Asian summer monsoon. *Geochimica et Cosmochimica Acta* **329**, 152–167.

Yu Y., Hathorne E., Siebert C., Gutjahr M., Fietzke J. and Frank M. (2024) Unravelling instrumental mass fractionation of MC-ICP-MS using neodymium isotopes. *Chemical Geology* **662**, 122220.

Yu Y., Siebert C., Fietzke J., Goepfert T., Hathorne E., Cao Z. and Frank M. (2020) The impact of MC-ICP-MS plasma conditions on the accuracy and precision of stable isotope measurements evaluated for barium isotopes. *Chemical Geology* **549**, 119697.

Zeng Z., Li X., Liu Y., Huang F. and Yu H.-M. (2019) High-precision barium isotope measurements of carbonates by MC-ICP-MS. *Geostandards and Geoanalytical Research* **43**, 291–300.